Climate Variability During Warm and Cold Phases of the Atlantic Multidecadal Oscillation (AMO) 1871-2008.

Michael A. Alexander[1], K. Halimeda Kilbourne[2], Janet A. Nye[3]

[1] NOAA/Earth System Research Laboratory, Boulder, CO 80305

[2] University of Maryland Center for Environmental Science, Chesapeake Biological Laboratory, Solomons, MD 20688

[3] School of Marine and Atmospheric Sciences, Stony Brook University, Stony Brook, NY 11794

For Submission to the Journal of Marine Systems

ICES AMO Special Issue

Submitted April 2012

Revised January 2013

Revised July 2013

Michael Alexander
NOAA/Earth System Research Laboratory
R/PSD1
325 Broadway
Boulder, CO 80305
Email: Michael.Alexander@noaa.gov
Phone: 1-303-433-9412
Fax: 1-303-4976449

Abstract

An extended reanalysis, a combination of observations and model output, is used to examine the spatial patterns of physical variables associated with the Atlantic Multidecadal Oscillation (AMO) from 1871-2008. The results are presented as anomalies during positive and negative phases of the AMO. As in previous studies, during positive (negative) AMO phases the sea surface temperature (SST) is anomalously warm (cold) over most of the North Atlantic, with the exception of the east coast of the United States. The atmospheric patterns associated with the positive phase of the AMO, include anomalous low pressure over the Atlantic between 20°S-50°N, cyclonic surface winds around the low, reduced wind speeds over the tropical Atlantic and enhanced precipitation in the eastern tropical Atlantic, with roughly opposite conditions during negative AMO phases. There are, however, substantial differences in the SST and the atmospheric anomalies between periods of the same phase, especially in the extratropics. Correlations between the AMO and air temperature anomalies are positive over much of the globe between 40°S and 50°N, with correlations exceeding 0.6 (~95% significance level) over the Maritime Continent and northern rim of the Pacific Ocean. Most of the sea level pressure (SLP) anomalies beyond the Atlantic are not statistically significant.

Highlights:

We investigated patterns of SST and atmospheric variability during phases of the AMO.

During positive AMO phases:

SST is anomalously warm over most of the North Atlantic;

low pressure extends over the Atlantic between 20°S-50°N;

wind speeds are reduced over the tropical Atlantic;

precipitation is enhanced in the eastern tropical Atlantic.

Roughly opposite conditions occur during the negative AMO phases.

There are substantial differences between periods, especially in the atmosphere.

Key Words: Ocean-atmosphere system; surface temperature; sea level pressure; atmospheric precipitations; reanalysis

Regional Terms: North Atlantic Ocean (0°-70°N, 80°W-10°E)

1. Introduction

The Atlantic Ocean exhibits variability over a wide range of temporal and spatial scales but has pronounced variability at decadal and multidecadal timescales. While there is an extensive history of studies on decadal variability in the North Atlantic (e.g. Bjerknes, 1964; Deser and Blackmon, 1993; Kushnir 1994; Schlesinger and Ramankutty, 1994), the term Atlantic Multidecadal Oscillation or AMO was first used in an editorial article by Kerr (2000) to describe slowly varying sea surface temperature (SST) anomalies that extend over most of the North Atlantic. The AMO is associated with the North Atlantic's dominant pattern of SST variability, with anomalies of the same sign over most of the basin but with larger anomalies in a horseshoe shape that includes the tropical Atlantic, the eastern portion of the entire basin, and from south of Greenland extending northwestward into the Labrador Sea. Over the past decade our knowledge of the AMO has increased greatly, including its evolution, spatial structure, potential causes, and impacts on climate and ecosystems (e.g. see Enfield et al., 2001; Lehodey et al., 2006; Delworth et al., 2007). Here we provide a brief background on the AMO and then examine its impact on climate during positive and negative phases of the AMO over ~140 years.

AMO indices have been calculated using a number of different methods (see Fig. 1 in Nigam et al., 2011, which presents several estimates of the AMO time series), but it has often been defined as the low-pass filtered SST anomaly averaged over the North Atlantic. The large-scale temperature changes over the North Atlantic are convolved with global climate change induced by an increase in greenhouse gases. Indeed the combined effects of anthropogenic climate change and the positive phase of the AMO since the

1990s may have caused a more rapid warming in the North Atlantic than would be expected from climate change alone (Andronova and Schlesinger, 2000; Belkin, 2009; Knudsen et al., 2011). Several different methods have been used to remove the anthropogenic signal including: linearly detrending the North Atlantic SSTs (Enfield et al., 2001; Sutton and Hodson, 2005), subtracting the global mean SST from the Atlantic SSTs (Trenberth and Shea, 2006), employing rotated Empirical Orthogonal Function analysis on the global SST field to separate the AMO from anthropogenic SST changes as well as from the influence of the Pacific on the Atlantic (Mestas-Nuñez, and Enfield, 1999; Guan and Nigam, 2009), and using twentieth century climate model simulations to define and then separate the externally forced (including greenhouse gasses) SST variations from the naturally varying component (Ting et al., 2009, Ting. et al., this issue).

The period of the AMO has been estimated to be 60-80 years (Schlesinger and Ranakutty, 1994; Delworth et al., 2007) but the length and consistency of the oscillation cycle is the subject of considerable debate. Given that there is ~160 years of SST data in the North Atlantic, only 1.5-2 cycles AMO cycles have been observed, making it impossible to determine whether this phenomena oscillates with a set periodicity. In addition, the method used to construct the AMO index as well as smoothing or detrending the SSTs results in oscillations of different frequencies (Vincze and Janosi, 2011). While paleoclimate data (Gray et al., 2004; Knudsen et al., 2011; Kilbourne et al., 2012) and climate models (Knight et al., 2005; Danabasoglu, 2008, Ting et al. 2009, this issue) provide additional evidence for the AMO, they also indicate that the oscillations are irregular with extended periods when they did not occur. Thus, Atlantic Multidecadal

Variability (AMV; Knight et al., 2005) rather than the AMO is perhaps more appropriate terminology for this phenomenon.

A wide variety of processes can contribute to decadal SST variability in the Atlantic, including: i) fluctuations in the surface heat fluxes (e.g. Chiang and Bitz, 2005) that can result in variability on decadal time scales when integrated over the deep winter mixed layer in the North Atlantic (Frankignoul and Hasselmann, 1977; Deser et al., 2003); ii) wind driven ocean currents that can result in decadal variability either by advection of the anomalies by the mean currents (e.g. Dickson et al., 1988; Hansen and Bezdek, 1996; Saravanan and McWilliams, 1998) or by the change in the strength or position of the ocean gyres and Gulf Stream (Frankignoul et al., 1997; Sturges et al., 1998); iii) decadal fluctuations in sea ice (Deser and Blackmon, 1993; Deser et al., 2002) and iv) changes in the strength of the Atlantic Meridional Overturning Circulation (AMOC) the Atlantic portion of the thermohaline circulation. As part of AMOC, water sinks in the Labrador Sea and other high latitude locations, flows south at depth over the entire length of the Atlantic Ocean and returns north at the surface, although the actual circulation is quite complex and involves eddies and recirculation gyres (Lozier, 2010). Other processes including anthropogenic warming, which slows the thermohaline circulation (IPCC, 2007), and solar and volcanic forcing (Otterä et al., 2010) can modulate AMOC and thus the AMO. Anthropogenic forcing may also contribute directly to low-frequency Atlantic SST variability due to non-linear greenhouse gas warming, and cooling during periods with increased manmade and/or natural aerosols (Mann and Emmanuel, 2006; Booth, et al., 2012).

While a range of factors influence multi-decadal Atlantic SST variability, the foremost hypothesis invokes fluctuations in the northward heat transported by AMOC to explain the AMO. Polyakov et al. (2005, 2009) linked the SST anomalies in the North Atlantic to multidecadal fluctuations in subsurface temperature and salinity that are consistent with changes in the overturning circulation. The subsurface data, however, are not of sufficient quantity and duration to determine multi-decadal oscillations in AMOC. Evidence for the link between the AMO and AMOC primarily comes from climate models, in which multidecadal variability in the overturning circulation over centuries long integrations results in Atlantic SST anomalies that resembles the AMO pattern. The timescale of the AMOC variability, however, varies between models and most have oscillations that are of shorter duration (~20-40 years) than the observed fluctuations in the AMO.

There are many competing hypotheses for oscillations in AMOC (see reviews by Delworth et al., 2007; Liu et al., 2012). For example, studies have found conflicting results as to whether anomalies in temperature, salinity, or both are critical for regulating sinking of dense water at high latitudes, a key component of AMOC variability. It is also unclear whether random atmospheric variability can force AMOC oscillations (e.g. Griffies and Bryan, 1997) or if atmosphere-ocean feedbacks are necessary for oscillations to occur (e.g. Timmerman et al. 1998).

The AMO exhibits positive (warm) and negative (cool) phases, where the difference between extremes is ~0.5°C (Fig. 1). Although the exact timing of the switch from a positive to negative phase depends on the data set used (Fig. 4) and how the index is calculated, negative/cold phases occurred from approximately 1900-1925 and 1965-1994

while positive/warm phases occurred from approximately 1875-1899, 1926-1965 and 1995-present. Positive phases of the AMO have been associated with low precipitation, droughts, reduced stream flow and elevated temperature in the southern US (Enfield et al., 2001; Sutton and Hodson, 2005, 2007, Nigam et al. 2011), but also with increased frequency and intensity of hurricanes (Goldenberg et al., 2001; Zhang and Delworth, 2006). Changes in ecosystem structure have been attributed to positive or negative phases of the AMO (see Nye et al. this issue).

Here we examine the spatial structure of SST and atmospheric anomalies during different phases of the AMO, focusing on the Atlantic sector but also including some global analyses. Our goal is to link the basin-scale AMO index to patterns of variability in the atmosphere and SST, so that oceanographers, meteorologists, and especially marine ecologists, may better gauge the regional expression of the AMO, its consistency between periods and its potential influence on ecosystem processes. In addition, the data source used here enables us to examine atmospheric fields over the ocean in the warm period in the late 19th century, whereas most previous AMO studies have either used data beginning in 1900 or focused on conditions over land.

2. Data and methods

2.1 20th century reanalysis

The atmospheric fields presented here are obtained from the "20th century reanalysis" (20CR; Compo et al., 2011), which actually extends from 1871 to 2008. Reanalyses, which combine observations with model-generated fields, are widely used in atmospheric and ocean sciences to study climate variability. Data assimilation uses statistical methods

to merge observations that are distributed irregularly in space and time, with an estimate of the state of the system given by a numerical model. While data assimilation systems are continually updated for initializing weather forecast models, a reanalysis uses the same assimilation method and model to reduce artificial discontinuities and thus are very useful for studying climate variability. Most reanalyses of the atmosphere begin after 1949 when upper air atmosphere measurements became available. The 20th century reanalysis only assimilates sea level pressure (SLP) measurements and so it can be extended back into the 19th century. SST and sea ice values were used as boundary conditions for the atmospheric model in 20CR are obtained from the HadISST data set (Rayner et al., 2003). The 20CR applies an advanced assimilation method, an ensemble Kalman filter, where the background error covariance necessary for estimating the state of the system, can vary with time. In the 20CR a set of 56 model simulations of the National Center for Environmental Prediction (NCEP) Global forecast system (GFS) model (experimental version circa April 2008) are used to estimate the error covariance matrix at six-hour intervals.

The 20CR output includes fields of atmospheric variables and an estimate of their uncertainty on a 2° latitude-longitude grid. The uncertainty arises from a lack of observations, measurement errors, model bias, and the finite number of ensemble members. The uncertainty tends to decrease as the density of observations increased from the 19th century through most of the 20th century. The uncertainty is also flow-dependent, e.g. it tends to be greater in regions of strong gradients, and differs among variables, e.g. the uncertainty is generally larger for precipitation than sea level pressure (Compo et al., 2011).

2.2 AMO definition

We calculated the AMO index following Enfield et al. (2001) by linearly detrending and applying a running 10-year mean to the monthly SST anomalies and then averaging the values over North Atlantic (0°-70°N, 80°W-10°E). The monthly anomalies are the deviations from the long-term monthly means over the entire 1871-2008 period obtained from the HadISST data set that had been interpolated to the 20CR reanalysis grid by Compo et al. (2011).

2.3 Additional data sets

In addition to the 20th century reanalysis/HadISST fields, the representation of the AMO and regional North Atlantic SST and air temperature anomalies are compared using additional data sets, including the: NOAA Extended Reconstruction SST (ERSST, version 3B, Smith et al., 2008), which now extends back to 1854; Kaplan extended SST version 2 (version 2; Kaplan et al., 1998); and SST and surface air temperature from the International Comprehensive Ocean-Atmosphere Data Set (ICOADS, Release 2.5, Woodruff et al., 2011). The datasets, including the HadISST, generally use the same SST observations obtained from merchant ships, research vessels and buoys, but with different processing. For example, in ICOADS observations are averaged within a grid square leaving regions without data as undefined, while sophisticated statistical methods are used to fill in data gaps in the ERSST and Kaplan datasets. The variable times series at each grid square from these datasets are linearly detrended prior to computing the anomalies in all of the analyses.

3. Results

3.1 North Atlantic

The AMO index clearly shows multi-decadal variability that is even apparent in the unfiltered monthly SST anomalies (Fig. 1). Based on Fig. 1 and previous studies of the AMO, we averaged the monthly anomalies over the following warm periods: 1871-1990, 1930-1963 and 1995-2008 and cold periods: 1905-1925 and 1968-1994. The epochs are separated by five years to avoid times when the AMO is near zero and its phase uncertain, except for the transition to the last epoch in the mid 1990s so the final warm period average could be as long as possible. The SST anomalies over the North Atlantic during these five periods are shown in Fig. 2 along with the long-term mean SST and the correlation between the AMO and 10-year running mean SST anomalies.

Consistent with the definition of the AMO, the sea surface temperature is above normal over much of the North Atlantic during the warm periods (Fig. 2 a,c,e) and below normal during the cold periods (Fig. 2 b,d). The anomaly pattern generally has a reverse "c" or horseshoe shape with positive values in the north tropical Atlantic, off the coast of Africa and Europe and across the basin between about 50°N-60°N during the three warm periods and negative values in these regions during the two cold periods. However, both the pattern and magnitude of the SST anomalies varies between periods. For example, the anomalies off the coast of the mid-Atlantic States (~35°N, 75°W) are near zero during 1871-1900, positive during 1930-1963, and negative during 1995-2008. In addition, there

is a tendency for the amplitude of the anomalies to increase over the period of record particularly to the east of Newfoundland, where they exceed 0.5°C in the last two epochs.

While the decadal SST anomalies may vary due to fluctuations in the strength and position of the Atlantic meridional overturning circulation and hence the AMO, several additional factors may influence the decadal SST anomalies including that: 1) the amount of data has generally increased through time and thus anomalies in the early part of the record may not have been recorded; 2) linearly de-trending the data may not remove all of the global warming signal, which then could be aliased into the AMO; 3) processes which may not be related to the AMO such as fluctuations in the gyres, persistence of anomalies due to the very deep mixed layers in the North Atlantic, atmospheric forcing that is random and/or is associated with teleconnections from other basins, etc.

The correlation between the AMO and local SST anomalies are shown in Fig. 1f. Even though there is 138 years of data, the very high autocorrelation in the AMO time series results in only ~6 degrees of freedom, which requires a correlation value of ~|0.6| to exceed the 95% confidence interval (e.g. Wilks, 1995). The AMO-SST correlations exceed 0.6 over much of the North Atlantic and reach 0.9 in a band extending from northeast of Brazil to the west of Portugal. In the Southern Hemisphere, positive correlations occur along the west coast of Africa but are near zero over the rest of the basin between about 5°-20°S.

The SST anomalies were filtered with a 12-month running mean for regions in the North Atlantic, East Atlantic and Tropical Atlantic (Fig. 3; the regions are denoted by grey rectangles in Fig. 2a). The multidecadal SST variability in all three regions closely tracks the AMO especially in the East and Tropical Atlantic regions, with the magnitude

of the anomalies on the order of 0.2°C. The main exception are the SST anomalies in the North Atlantic region which exhibit an amplified multi-decadal oscillation since ~1960. Fluctuations on shorter time scales are readily apparent from the 12-month running mean values, with amplitudes of up to 0.8°C in the North Atlantic region. Previous studies have indicated strong decadal (9-15 year) variability south of Greenland (Deser and Blackmon, 1993; Deser et al., 2002). As a result, short-term averages may not provide an accurate representation of variability associated with the AMO; for example negative SST anomalies occur in the North Atlantic region during the late 1940s in the middle of an AMO warm period. In addition, if measurements are taken infrequently, then shorter period SST variability may be aliased into estimates of the regional AMO signal. Aliasing may be of greater concern for some biological and subsurface ocean variables, which are measured less frequently than SST.

One measure of uncertainty in the AMO and the related regional SST anomalies is how they differ across data sets. The AMO and 10-year running mean SST time series in the Tropical, East and North Atlantic regions obtained from the ERSST, Kaplan, and ICOADS are presented in Fig. 4, along with the HadISST time series (repeated from Fig. 3). Whereas all of the time series show the decadal warm and cold periods associated with fluctuations in the AMO, differences in the magnitude of the anomalies and temporal evolution, especially for the Northern Region, are readily apparent. For example, the zero crossings for the AMO and the three regional SST time series differ by as much as five years between datasets. The ICOADS air temperature anomalies averaged over the entire North Atlantic (AMO region) as well as for the three sub regions are also shown (as magenta lines) in Fig. 4. While the air temperature time series confirm

the warm and cold epochs associated with the AMO, they are more variable and depict a negative anomaly around 1910 that is much more pronounced than in the SST data. In addition to responding to the AMO, air temperatures over the North Atlantic are strongly influenced by other factors such as the North Atlantic Oscillation (NAO), local conditions and random weather related fluctuations, which contribute to variability even on decadal time scales.

The AMO and its impact on climate can vary with the seasonal cycle, for example the AMO appears to have the strongest impact on precipitation over North America during summer (e.g. Nigam et al. 2011). We explore the seasonal influence of the AMO on the ocean in Fig. 5, which shows the (unfiltered) SST anomalies as a function of calendar month averaged over the years in each of the five epochs for the Tropical, East and North Atlantic regions. The mean seasonal cycle of SSTs over the entire record (1871-2008) are also shown in Fig 5 for the three regions. (The mean and anomalous SSTs are shown separately because the anomalies are small and thus the total SST values in each epoch nearly overlap each other.) The mean seasonal cycle increases in amplitude with the latitude of the region, i.e. it is approximately 1.25, 2.5 and 4 °C for the Tropical, East and North Atlantic regions, respectively. In general the SST anomalies in each epoch are positive during warm epochs and negative in cold in all 12 calendar months, with the exception of those averaged over 1905-1925 and 1930-1963 during May and in 1871-1900 during July-September in the North Atlantic region (Fig. 5), reflecting the greater non-AMO related variability there (highlighted in Fig 3). The anomalies in the Tropical and East Atlantic regions, while exhibiting some variability as a function of season, are fairly uniform with absolute values of 0.05 to 0.3°C. Although the sample size is small,

the results suggest that the small positive AMO-related change in temperatures over the course of the year, would result in a slightly earlier occurrence of thermal spring over most of the North Atlantic in warm epochs and the reverse in cold epochs.

The sea level pressure anomalies during all five periods are shown in Fig. 6. The magnitude of the anomalies ranges from 0.1-1.0 mb with anomalously low pressure over the tropics in both hemispheres that extends to ~45°N over the North Atlantic during the warm periods (Fig. 6a, c, e) and high pressure over these regions during the cold periods (Fig. 6b, d). These tropical anomalies are consistent with the model response to specified AMO-derived SST anomalies in the North Atlantic (Sutton and Hodson, 2007; Delworth et al., 2007). The spatial structure of the SLP anomalies is similar during the warm periods of 1871-1900 and 1995-2008 exhibiting a meridional dipole with negative anomalies between 20°N-45°N and positive anomalies north of 50°N. The cold period of 1905-1925 has a similar pattern but with the signs reversed. The anomaly pattern during these three periods resembles the North Atlantic Oscillation (NAO), a north-south dipole in sea level pressure. Some climate modeling experiments indicate a link between AMOC/AMO and the NAO, but the exact mechanism, including whether the whether the NAO drives or responds to the AMO and the resulting lead/lag relationship between the two, depends on the study (e.g. Danabasoglu et al., 2012; Kwon and Frankignoul, 2011; Gastineau and Frankignoul, 2012).

The SLP anomaly pattern is quite different during the warm epoch of 1930-1963 and the cold epoch of 1968-1994, when anomalies of the same sign cover most of the North Atlantic with maximum amplitude near 55°N in the eastern half of the basin (Fig. 6). It is unclear why the SLP anomalies during these two periods have similar patterns (with the

opposite sign) but differ from the meridional dipole structure during the other three periods. There is not an obvious link to the SSTs that occurred during 1930-1963 and 1968-1994 (Fig. 2) that would cause the SLP anomalies to differ during these epochs. Other factors besides the AMO-related SST anomalies influence the atmosphere over the North Atlantic, including SSTs in other ocean basins, sea-ice anomalies and especially variations due solely to atmospheric processes. For example, differences in sea-ice concentration can influence atmospheric anomalies (e.g. Alexander et al., 2004), and the spread among atmospheric model simulations to the same prescribed SSTs indicates that internal atmospheric variability can obscure the atmospheric response to the ocean and ice anomalies (e.g. Alexander et al., 2002; Alexander et al., 2004).

The long-term mean SLP and the correlation between the AMO and the grid values of the low-pass filtered SLP anomalies are shown in Fig. 6f. The mean pressure pattern depicts the subtropical high centered at 35°N, 30°W and the Icelandic low at 60°N, 35°W. The negative correlations between the AMO and SLP are significant (< -0.6) on the eastern side of the subtropical North Atlantic. Thus, warm SSTs associated with the positive phase of the AMO results in negative SLP anomalies that weaken the subtropical high.

The anomalous surface wind direction (gray arrows) and surface wind speed anomalies (shading/contours) for each of the five periods along with the mean wind direction and the correlation between the AMO and the wind speed are shown in Fig. 7. The anomalous winds are from the west over the Atlantic between approximately 0°-20°N during the warm periods (Fig. 7a, c, e) and from the east during the cold periods (Fig. 7b, d). Since the mean trade winds blow from east to west over most of the tropical

Atlantic (Fig. 7f), the anomalies oppose the mean winds during warm periods and increase the winds during cold periods, resulting in negative correlations between the AMO and wind speed across the Atlantic between 0°-20°N (Fig. 7f). The circulation is cyclonic (counterclockwise in the Northern Hemisphere) over the eastern subtropical Atlantic during the three warm periods and anticyclonic during the two cold periods. The center of these circulation anomalies is somewhat variable between periods but is generally located in the vicinity of 20°N, 30°W. As anticipated, extratropical winds follow the geostrophic relationship with cyclonic (anticyclonic) circulation (Fig. 7a-e) around low (high) pressure systems (Fig 6a-e). Compared to the tropics, the wind speed anomalies in the middle and high latitudes are more variable between periods as they are more strongly influenced by internal atmospheric processes. While ocean currents associated with the Atlantic meridional overturning circulation may still maintain warm SSTs, the anomalous extratropical winds are very different during 1930-1963 compared to the other two warm periods. For example, they are stronger and from the northwest over the Labrador Sea during 1930-1963 in contrast to anomalous winds from the east/southeast during 1871-1900 and 1995-2008. The associated net surface heat fluxes cool the underlying ocean (not shown), and along with wind-driven currents, may explain why the Labrador Sea exhibits little overall warming, and even negative SST anomalies over the eastern portion of the Sea, during 1930-1963 (Fig. 2c).

The precipitation anomalies during the five epochs generally show enhanced precipitation between 0°-20°N in the eastern Atlantic during warm AMO periods (Fig. 8a, c, e) and decreased precipitation during cold periods (Fig. 8b, d). In addition, there is some tendency for the anomalies over the tropical Atlantic in the Southern Hemisphere to

be of opposite sign to those to north of the equator but not during every epoch. The amplitude of the anomalies is on the order of 0.1-0.6 mm day^{-1}. Correlations between the AMO and the local precipitation (Fig. 8f) exceed the 95% significance level of 0.6 in the vicinity of 15°N, 25°W. Given that the annual mean precipitation over the Atlantic is concentrated in the Intertropical Convergence Zone (ITCZ) between approximately 5°S-10°N (Fig. 8f), the structure of the anomalies indicate a northward shift of the ITCZ.

The precipitation anomalies beyond the tropical Atlantic are more variable and it is difficult to discern a clear relationship with the phase of the AMO. The correlation pattern (Fig. 8) suggests enhanced precipitation over the Sahel (across Africa between 10°-20°N) and reduced precipitation over equatorial Africa and the eastern United States south of ~45°N except for southern Florida. These signals, albeit weak, are consistent with previous studies linking the AMO to continental precipitation (e.g. Folland et al., 1986; Enfield et al., 2001; Zhang and Delworth, 2006; Ting et al., 2011; Nigam et al., 2011).

3.2 Global AMO signal

While the AMO is centered in the Atlantic its influence may well extend to the Arctic, Pacific Ocean and other parts of the globe (e.g. see Enfield et al., 2001; Knight et al., 2005; Zhang and Delworth, 2007; Chylek et al., 2009). The link between multidecadal North Atlantic SST fluctuations and atmospheric variability is examined via correlations and regressions between the AMO and both sea level pressure and surface air temperature (SAT) from the 20CR (Fig. 9). While correlation and regressions provide related information, one can better gauge the robustness of the relationship from

correlations but the magnitude of the change (relative to the AMO) from regressions. The variables were first low-pass filtered using a 10-year running mean. The results are presented for the globe north of 40°S, due to a lack of observations over the Southern Oceans and Antarctica, although AMO-related SST anomalies in the Southern Ocean appear to be out of phase with those in the North Atlantic (e.g. Deser et al., 2010).

The AMO-SLP correlations and regressions, indicate warm SSTs in the Atlantic are associated with low pressure (negative values) over the subtropical South Atlantic as well as the North Atlantic where the latter extend eastward over nearly all of Africa, across southern Asia and the northern Indian Ocean, and over the Maritime Continent. Low pressure also occurs over the northeast Pacific. The AMO is associated with anomalously high pressure over eastern Asia, the Rocky Mountains, the Arctic and portions of the Southern Ocean. However, the correlations are generally below 0.6 (the 95% confidence interval) outside the north tropical Atlantic and northern Indian Ocean, and the magnitude of the regressions is generally less than 2 mb per °C change in the AMO in midlatitudes and 4 mb per °C over the Arctic.

The correlation between the AMO and SAT anomalies is positive over much of the globe between 40°S and 50°N, with correlations exceeding 0.6 over the Maritime Continent/western tropical Pacific and the northern rim of the Pacific. The main exception is the central equatorial Pacific, which has a weak negative relationship with the AMO. SST variability in the central and eastern equatorial Pacific is mainly controlled by El Nino and the Southern Oscillation (ENSO), rather than the AMO, even on decadal time scales. However, surface air/sea temperature anomalies (SST and the overlying SAT are strongly correlated at seasonal and longer time scales) in the west

Pacific, influence the winds and SSTs in the central Pacific; e.g. when temperatures are warmer in the west, the easterly trade winds increase over the equator in the central Pacific enhancing upwelling thereby cooling the SST and SAT. This process may lead to the modest negative correlation between the AMO and temperature anomalies in the central and eastern equatorial Pacific. While these correlations are not statistically significant, they are consistent with the observational analysis of Deser et al. (2010), as well as the modeling study of Zhang and Delworth (2005) who found that a decrease in AMOC and the associated cold AMO-like SSTs in the North Atlantic resulted in El Niño conditions in the tropical Pacific. The regression between the AMO and SAT are greater over continents and the Arctic compared with the ocean, due to the moderating influence of the oceans on air temperature variability. The magnitude of the regression coefficients exceeds 2°C per °C AMO change in some locations including central North America, although the pattern is noisy and may reflect unrelated local variability (large amplitude but low correlation).

4. Summary and Discussion

Our analysis of a recently developed extended reanalysis explores the spatial and temporal patterns of SST and atmospheric variables associated with the AMO. The AMO-related North Atlantic sea surface temperature anomalies are warm during 1871-1900, 1930-1963, 1995-2008 and cold during 1905-1925, 1968-1994. The SST anomalies are fairly consistent over the course of the seasonal cycle within an epoch, i.e. the period mean anomalies are nearly all positive (negative) during all calendar months in a warm (cold) epoch, but the pattern and amplitude of the anomalies clearly differ between

epochs. Decadal SST anomalies in regions of the tropical Atlantic, eastern Atlantic, and North Atlantic vary with the AMO, and the regional SST time series are fairly similar when obtained from different datasets. However, there are some differences in estimates of SST variability, e.g. the timing of the zero crossing can vary by as much as ~5 years between datasets. The SST anomalies differ most between data sets in the North Atlantic region (located east of Newfoundland), and air temperature anomalies exhibit more irregular behavior than the underlying SST in all of the regions and may not reflect AMO-related variability in some periods.

Results from previous studies suggest that changes in the strength of the Atlantic meridional overturning circulation results in AMO-related SSTs over much of the North Atlantic. While some of the SST differences between periods may reflect fluctuations in the overturning circulation, processes that are independent of AMOC, such as anthropogenic forcing, NAO and ENSO variability, likely contribute to these differences.

The atmospheric patterns associated with the positive phase of the AMO, include anomalous low pressure over the Atlantic between 20°S-50°N, cyclonic surface winds around the low, reduced wind speeds over the tropical Atlantic and enhanced precipitation in the eastern tropical Atlantic, with roughly opposite conditions during the negative phase of the AMO. The atmospheric anomalies are much more variable between periods at mid and high latitudes. The atmospheric response to these anomalies is most consistent in the tropics, where positive SST anomalies lead to enhanced precipitation and a low pressure system poleward of the precipitation. While both tropical and extratropical SST anomalies can influence the atmosphere (e.g. Sutton and Hodson, 2007), the response is generally not as robust to the latter and internal atmospheric

variability is greater in mid and high latitudes resulting in a lower signal-to-noise ratio in the extratropics relative to the tropics. The AMO-related sensible, latent, shortwave and longwave surface heat flux anomalies in both the tropics and midlatitudes (not shown) are not consistent across epochs, and have small spatial scales and modest amplitudes (< 5 Wm^{-2}). Given that estimates of the surface heat fluxes, which depend on the surface wind speed, air-sea temperature difference and clouds, are known to have sizeable errors (e.g. Kubota et al., 2008; Smith et al., 2011; Kent et al., 2012), uncertainty in the fluxes may well exceed their AMO signal.

The correlation between the AMO and air temperature anomalies is positive over much of the globe between 40°S and 50°N, with correlations exceeding 0.6 (~95% significance level) over the Maritime Continent/western tropical Pacific Ocean and the subarctic portion of the Pacific. The positive phase of the AMO is associated with low pressure over the subtropical South Atlantic and in a band extending from the North Atlantic eastward to the tropical West Pacific. However, most of the AMO-SLP correlation values are not statistically significant outside of the North Atlantic between 0°-40°N and a portion of the northern Indian Ocean.

While the data suggest that the AMO SST signal is coherent and long lived over much of the North Atlantic, it is relatively small in amplitude. For example, the AMO-related SST anomalies are on the order of ~0.2°C; in contrast, SST anomalies associated with the Pacific Decadal Oscillation (PDO) and ENSO can exceed 0.5°C and 1°C, respectively (e.g. Mantua et al., 1997; Deser et al., 2010). Thus it may be difficult to determine the AMO-driven processes that impact ecosystems, as they may be subtle and/or not directly related to the local temperature (see Nye at al., this issue). In addition,

the long periods involved in the AMO and the short duration of most biological measurements could lead to a fortuitous correspondence between the two that does not continue over time. This concern is heightened if the biological quantity under consideration also exhibits slow variations, e.g. for species which grow and reproduce slowly.

Acknowledgements

We thank Gil Compo for his assistance in obtaining and interpreting the 20th century reanalysis data. We also thank Clara Deser and Jamie Scott for their suggestions for improving the manuscript and the presentation of the figures. This is contribution No. 4773 of the University of Maryland Center for Environmental Science.

References

Alexander, M.A., Bhatt, U.S., Walsh, J.E., Timlin, M.S., Miller, J.S., Scott, J.D., 2004. The atmospheric response to realistic Arctic sea ice anomalies in an AGCM during Winter. J. Climate, 17, 890-905.

Alexander, M.A., Blade, I., Newman, M., Lanzante, J.R., Lau, N.-C., Scott, J.D., 2002. The atmospheric bridge: the influence of ENSO teleconnections on air-sea interaction over the global oceans. J. Climate, 15, 2205-2231.

Andronova, N.G., Schlesinger, M.E., 2000. Causes of global temperature changes during the 19th and 20th centuries. Geophys. Res. Lett., 27, 2137-2140.

Belkin, I.M., 2009. Rapid warming of Large Marine Ecosystems. Prog. Oceanogr., 81, 207-213.

Bjerknes, J., 1964. Atlantic air-sea interaction. Adv. Geophys. **20**: 1-82.

Booth, B.B.B., Dunstone, N.J., Halloran, P.R., Andrews, T., Bellouin, N., 2012. Aerosols implicated as a prime driver of twentieth-century North Atlantic climate variability. Nature, 484, 228–232.

Chiang, J.C.H., Bitz, C.M., 2005. Influence of high latitude ice cover on the marine Intertropical Convergence Zone. Clim. Dyn., 25, 477-496. DOI: 10.1007/s00382-005-0040-5.

Chylek, P., Folland, C., Lesins, G., Dubey, M., Wang, M., 2009. Arctic air temperature change amplification and the Atlantic Multidecadal Oscillation. Geophys. Res. Lett., 36, L14801, doi: 10.1029/2009GL038777.

Compo, G. P., Whitaker, J. S., Sardeshmukh, P. D., Matsui, N., Allan, R. J., Yin, X., Gleason, B. E., Vose, R. S., Rutledge, G., Bessemoulin, P., Brönnimann, S., Brunet, M., Crouthamel, R. I., Grant, A. N., Groisman, P. Y., Jones, P. D., Kruk, M., Kruger, A. C., Marshall, G. J., Maugeri, M., Mok, H. Y., Nordli, Ø., Ross, T. F., Trigo, R. M., Wang, X. L. Woodruff, S. D., Worley, S. J. 2011, The Twentieth Century Reanalysis Project. Quart. J. Roy. Met. Soc., 137, 1–28, doi:10.1002/qj.776.

Danabasoglu, G., 2008. On Multidecadal Variability of the Atlantic Meridional Overturning Circulation in the Community Climate System Model Version 3. J. Climate, 21, 5524–5544.doi: http://dx.doi.org/10.1175/2008JCLI2019.1

Danabasoglu, G., S. G. Yeager, Y.-O. Kwon, J. J. Tribbia, A. S. Phillips, J. W. Hurrell, 2012. Variability of the Atlantic Meridional Overturning Circulation in CCSM4. J. Climate, 25, 5153–5172. doi: http://dx.doi.org/10.1175/JCLI-D-11-00463.1

Delworth, T.L., Zhang, R., Mann, M.E., 2007. Decadal to centennial variability of the Atlantic from observations and models In Ocean Circulation: Mechanisms and Impacts. Geophysical Monograph Series 173, Washington, DC, American Geophysical Union, 131-148.

Deser, C., Blackmon, M., 1993. Surface climate variations over the North Atlantic Ocean during winter: 1900-1989. J. Climate, 6, 1743-1753.

Deser, C., Alexander, M.A., Timlin, M.S., 2003. Understanding the persistence of sea surface temperature anomalies in midlatitudes. J. Climate, 16, 57-72.

Deser, C., Alexander, M.A., Xie, S.-P., Phillips, A.S., 2010. Sea Surface Temperature Variability: Patterns and Mechanisms. Ann. Rev. Mar. Sci., 2, 115-143, doi:10.1146/annurev-marine-120408-151453.

Deser, C., Holand, M., Reverdin, G., Timlin, M.S., 2002. Decadal variations in Labrador sea ice cover and North Atlantic sea surface temperatures. J. Geophys. Res., 107, C5, doi:10.1029/2000JC000683.

Dickson, R. R., J. Meincke, S.-A. Malmberg, A. J. Lee, 1988. The “Great Salinity Anomaly” in the northern North Atlantic, 1968–1982, Prog. Oceanogr., 20, 103–151.

Enfield, D.B., Mestas-Nunez, A.M., Trimble, P.J. 2001. The Atlantic multidecadal oscillation and its relation to rainfall and river flows in the continental U.S. Geophys. Res. Lett., 28(10): 2077-2080.

Folland, C. K., Palmer, T.N., Parker, D.E., 1986. Sahel rainfall and worldwide sea temperatures, 1901–85. Nature, 320, 602–607.

Frankignoul, C., Hasselmann, K., 1977. Stochastic climate models. Part 2. Application to sea-surface temperature variability and thermocline variability. Tellus, 29, 289–305.

Frankignoul, C., Muller, P., Zorita, E., 1997. A simple model of the decadal response of the ocean to stochastic wind forcing. J. Phys. Oceanogr., 27, 1533–1546.

Gastineau, G., C. Frankignoul, 2012. Cold-season atmospheric response to the natural variability of the Atlantic meridional overturning circulation. Clim. Dyn., 39, 10.1007/s00382-011-1109-y.

Goldenberg, S.B., Landsea, C.W., Mestas-Nunez, A.M., Gray, W.M., 2001. The recent increase in Atlantic hurricane activity: causes and implications. Science, 293, 474-479.

Gray, S.T., Graumlich, L.J., Betancourt, J.L., Pederson, G.T., 2004. A tree-ring based reconstruction of the Atlantic Multidecadal Oscillation since 1567 A.D. Geophys. Res. Lett., 31, L12205, doi:10.1029/2004GL019932.

Griffies, S. M., K. Bryan, 1997: Predictability of North Atlantic multidecadal climate variability. *Science*, 275(5297), 181-184.

Guan, B., Nigam S., 2009. Analysis of Atlantic SST variability factoring inter-basin links and the secular trend: Clarified structure of the Atlantic Multidecadal Oscillation. J. Climate, 22, 4228–4240, doi:10.1175/ 2009JCLI2921.1.

Hansen, D., Bezdek, H., 1996. On the nature of decadal anomalies in North Atlantic sea surface temperature. J. Geophys. Res., 101(C4): doi: 10.1029/95JC03841. issn: 0148-0227.

IPCC, 2007. Climate Change 2007: The Physical Science Basis. Contribution of Working Group I to the Fourth Assessment Report of the Intergovernmental Panel on Climate Change. Solomon, S., Qin, S., Manning, M., Chen, Z., Marquis, M., Averyt, K.B. Tignor, M., Miller, H.L. (Eds.). Cambridge University Press, Cambridge, United Kingdom and New York, NY, USA.

Kaplan, A., M. Cane, Y. Kushnir, A. Clement, M. Blumenthal, B. Rajagopalan, 1998. Analyses of global sea surface temperature 1856-1991, J. of Geophys. Res., 103, 18,567-18,589.

Kent, E. C., Fangohr, S., D. I. Berry, 2012, A comparative assessment of monthly mean wind speed products over the global ocean. Int. J. Climatol.. doi: 10.1002/joc.3606

Kerr, R.A., 2000. A North Atlantic climate pacemaker for the centuries. Science, 288 (5473): 1984–1986.

Kilbourne, K.H., Alexander, M.A., Nye, J. 2012. Paleoclimate perspective on Atlantic multidecadal variability. J. Mar. Syst., this issue.

Knight, J.R., Allan, R.A., Folland, C.K., Vellinga, M., Mann, M.E., 2005. A Signature of persistent natural thermohaline circulation cycles in observed climate. Geophys. Res. Let. , 32, L20708, doi:10.1029/2005GL024233, 2005.

Knudsen, M.F., Seidenkrantz, M.-S., Jacobsen, B.H., Kuijpers, A., 2011. Tracking the Atlantic Multidecadal Oscialltion through the last 8000 years. Nature Communications, 2, 1-8.

Kubota, M., N. Iwabe, M. F. Cronin, H. Tomita, 2008. Surface heat fluxes from the NCEP/NCAR and NCEP/DOE reanalyses at the Kuroshio Extension Observatory buoy site, J. Geophys. Res., 113, C02009, doi:10.1029/2007JC004338.

Kushnir, Y., Interdecadal Variations in North Atlantic Sea Surface Temperature and Associated Atmospheric Conditions, 1994. J. Climate, 7, 141- 157.

Kwon Y-O, Frankignoul C., 2011. Stochastically-driven multidecadal variability of the Atlantic meridional overturning circulation in CCSM3. Clim. Dyn. 38, 859–876. doi:10.1007/s00382-011-1040-2.

Lehodey, P., Alheit, J., Barange, M., Baumgartner, T., Beaugrand, G., Drinkwater, K., Fromentin, J.-M., Hare, S. R., Ottersen, G., Perry, R. I., Roy, C., van der Lingen, C. D., Werner, F., 2006. Climate variability, fish, and fisheries. J. Climate, 19, 5009-5030.

Liu, Z., 2012. Dynamics of Interdecadal Climate Variability: A historical perspective. J. Climate, 25, 1963–1995.

Lozier, M.S., 2010: Deconstructing the Conveyor Belt, Science, 328, 1507-1511.

Mann, M.E., Emanuel, K.A., 2006. Atlantic hurricane trends linked to climate change. EOS, 87, 233-244.

Mantua, N.J., Hare, S. R., Zhang, Y., Wallace, J.M., Francis, R., 1997. A Pacific interdecadal climate oscillation with impacts on salmon production. Bull. Amer. Meteor. Soc., 78, 1069-1079.

Mestas-Nuñez, A.M., Enfield, D.B., 1999. Rotated Global Modes of Non-ENSO Sea Surface Temperature Variability. J. Climate, 12, 2734–2746.

Nigam, S., Guan, B., Ruiz-Barradas A., 2011. Key role of the Atlantic Multidecadal Oscillation in 20th century drought and wet periods over the Great Plains. Geophys. Res. Lett., 38, L16713, doi:10.1029/2011GL048650.

Nye, J.A., Kenny, A., Kilbourne, K.H., VanHoutan, K.S., Stachura, M., Baker, M., Bell, R., Martino, E., 2013. Ecosystem effects of the Atlantic Multidecadal Oscillation. J. Mar. Syst. This issue.

Otterä, O. H., Bentsen, M., Drange, H., and Suo, L.L., 2010. External forcing as a metronome for Atlantic multidecadal variability, Nature Geoscience, *3*(10), 688-694.

Polyakov, I.V., Alexeev, V.A., Bhatt, U.S., Polyakova, E.V., Zhang, X., 2009. North Atlantic warming: Patterns of long-term trend and multidecadal variability. Climate Dynamics, DOI 10.1007/s00382-008-0522-3.

Polyakov I.V., Bhatt, U.S., Simmons, H.L., Walsh, D., Walsh, J.E., Zhang, X., 2005. Multidecadal Variability of North Atlantic Temperature and Salinity during the Twentieth Century. J. Climate, 18, 4562-4581.

Rayner, N.A., Parker, D.E., Horton, E.B., Folland, C.K., Alexander, L.V., Rowell, D.P., Kent, E.C., Kaplan, A., 2003. Global analyses of sea surface temperature, sea ice, and night marine air temperature since the late nineteenth century, J. Geophys. Res., 108, 4407, doi:10.1029/2002JD002670.

Saravanan, R., J.C. McWilliams, 1998. Advective ocean--atmosphere interaction: an analytical stochastic model with implications for decadal variability. J. Climate, 11, 165-188.

Schlesinger, M.E., N. Ramankutty, 1994. An oscillation in the global climate system of period 65-70 years. Nature, 367, 723-726.

Smith, S. R., P.J. Hughes, M.A. Bourassa, 2011. A comparison of nine monthly air–sea flux products. Int. J. Climatol., 31, 1002–1027. doi: 10.1002/joc.2225

Smith, T.M., R.W. Reynolds, T. C. Peterson, J. Lawrimore, 2008. Improvements to NOAA's Historical Merged Land-Ocean Surface Temperature Analysis (1880-2006). J. Climate, 21, 2283-2296

Sutton, R.T., Hodson, D.L.R., 2005. Atlantic Ocean forcing of North American and European summer climate. Science, 309, 115-118.

Sutton, R.T., Hodson, D.L.R., 2007. Climate response to Basin-Scale Warming and Cooling of the North Atlantic Ocean. J. Climate, 20, 891-907.

Sturges, W., Hong, B.G., Clarke, A.J., 1998. Decadal Wind Forcing of the North Atlantic Subtropical Gyre. J. Phys. Oceanogr., 28, 659–668.

Timmermann, A., M. Latif, R. Voss, A. Grötzner, 1998. Northern Hemispheric Interdecadal Variability: A Coupled Air-Sea Mode, J. Climate, 12, 2607-2624.

Ting, M., Kushnir, Y., Li, C., 2013. North Atlantic multidecadal SST variability: external forcing versus internal variability. J. Mar. Syst. This issue.

Ting, M., Kushnir, Y., Seager, R., Cuihua, L., 2011. Robust features of Atlantic multi-decadal variability and its climate impacts. Geophys. Res. Lett., 38(L17705): doi:10.1029/2011GL048712.

Ting, M., Kushnir, Y., Seager, R., Li, C., 2009. Forced and internal twentieth-century SST trends in the North Atlantic. J. Clim., 22, 1469–1481, doi:10.1175/2008JCLI2561.1.

Trenberth, K.E., Shea, D.J., 2006. Atlantic hurricanes and natural variability in 2005, Geophys. Res. Lett., 33, L12704, doi:10.1029/2006GL026894.

Vincze, M., Janosi, I.M., 2011. Is the Atlantic Multidecadal Oscillation (AMO) a statistical phantom? Nonlinear Processes in Geophys., 18, 469-475.

Wilks, D.S., 1995. Statistical Methods in the Atmospheric Sciences. 59 International Geophysics Series, Academic Press, San Diego, 467 pp.

Woodruff, S.D., S.J. Worley, S.J. Lubker, Z. Ji, J.E. Freeman, D.I. Berry, P. Brohan, E.C. Kent, R.W. Reynolds, S.R. Smith, C. Wilkinson, 2011. ICOADS Release 2.5: Extensions and enhancements to the surface marine meteorological archive. Int. J. Climatol. (CLIMAR-III Special Issue), **31**, 951-967 (doi:10.1002/joc.2103).

Zhang, R., T.L. Delworth, 2005. Simulated tropical response to a substantial weakening of the Atlantic thermohaline circulation**.** J. Climate, 18, doi:10.1175/JCLI3460.1.

Zhang, R., Delworth, T.L., 2006. Impact of Atlantic multidecadal oscillations on India/Sahel rainfall and Atlantic hurricanes. *Geophys. Res. Lett.*, 33, L17712, doi:10.1029/2006GL026267.

Zhang, R., Delworth, T.L., 2007. Impact of the Atlantic Multidecadal Oscillation on North Pacific climate variability. Geophys. Res. Let., 34, L23708,doi:10.1029/2007GL031601.

Figure Captions

Fig. 1. AMO time series as obtained from the linearly detrended SST Anomalies (°C) averaged over the entire North Atlantic (0°-70°N, 80°W-10°E) calculated using the 10-year running mean (black line). Monthly anomalies are shown by the grey line. SSTs are obtained from the HadISST data set (Rayner et al., 2003).

Fig. 2. The sea surface temperature anomalies relative to the 1871-2008 average for the periods (a) 1871-1900, (b) 1905-1925, (c) 1930-1963, (d) 1968-1994 and (e) 1995-2008. The three positive-phase AMO periods are shown in (a), (c) and (e), and the negative phase periods in panels (b) and (d). The anomalies, based on de-trended data, are shown as both contours (interval is 0.1 °C) and shading (interval of 0.05, scale on right of panel d). (f) Long term mean SST (contoured interval 5°C) and the correlation between the AMO and the 10-year running mean SST (shading interval 0.1, scale on right of panel f).

Fig. 3. SST anomalies (°C) averaged over the North Atlantic (40°-60°N, 60°-30°W), Eastern Atlantic (20°-60°N, 30°W-0°) and tropical Atlantic (0°-20°N, 80°W-10°W) regions (gray rectangles in Fig. 2a): 12-month running mean (grey shading), 10-year running mean and AMO time series.

Fig. 4. Time series of the AMO and the de-trended 10-year running average of SST anomalies in the Tropical Atlantic, East Atlantic and North Atlantic regions from the following datasets: HadISST (blue, repeated from Fig. 3); ERSST (red); Kaplan (green); ICOADS (black). Also shown are the anomalous air temperature time series (purple) averaged over the entire North Atlantic (AMO region) as well as for the three smaller regions. The datasets are described in section 2.

Fig. 5. The seasonal cycle of the long term mean SSTs and the average SST anomalies in each of the 5 epochs in the Tropical, East and North Atlantic regions. The mean SSTs (black line without symbols, scale on right) are based on monthly values averaged over 1871-2008. The unfiltered monthly SST anomalies in the warm and cold epochs are shown for: 1871-1900 (crosses); 1905-1925 (open circles); 1930-1963 (x); 1968-1994 (open squares); 1995-2008 (filled squares), with the scale on the left. Note the scales of both the mean and epoch anomalies differ between regions.

Fig. 6. As in Fig. 2, but for SLP anomalies. The anomalies are shown as both contours (interval is 0.2 mb) and shading (interval of 0.1 mb, scale on right of panel d). (f) Long term mean SLP (contours interval 4 mb) and the correlation between the AMO and the 10-year running mean SLP (shading interval 0.1, scale on right of panel f).

Fig. 7. As in Fig 2 but for the surface wind. (a)-(e) anomalous wind direction (gray equal length vectors) and anomalous wind speed shown by both contours (0.1 m sec) and shading (scale to the right of panel d 0.05 m/sec) for the five periods. (f) Mean wind direction (grey vectors, mean wind speed (contours), correlation between the AMO and the 10-year running mean wind speed (shading, scale on right).

Fig. 8. As in Fig. 2, but for the precipitation. The anomalies are shown as both contours (interval is 0.2 mm day^{-1}) and shading (interval of 0.05 mm day^{-1}, scale on right of panel d). (f) Long term mean precipitation (contours interval 1 mm day^{-1}) and the correlation between the AMO and the 10-year running mean precipitation (shading interval 0.1, scale on right of panel f).

Fig. 9. Correlations between the AMO index and (a) sea level pressure (SLP) and (c) surface air temperature (SAT); regressions of (b) SLP and (d) SAT on the AMO. All variables have been de-trended and smoothed with a 10-year running. The contour intervals are (a) 0.2, (b) 1.0 mb $°C^{-1}$, (c) 0.2, and (d) 0.5°C per $°C^{-1}$ change in the AMO. Absolute correlation (regression) values of 0.6 and 0.8 (1 and 2) are shaded and have thicker contour lines.

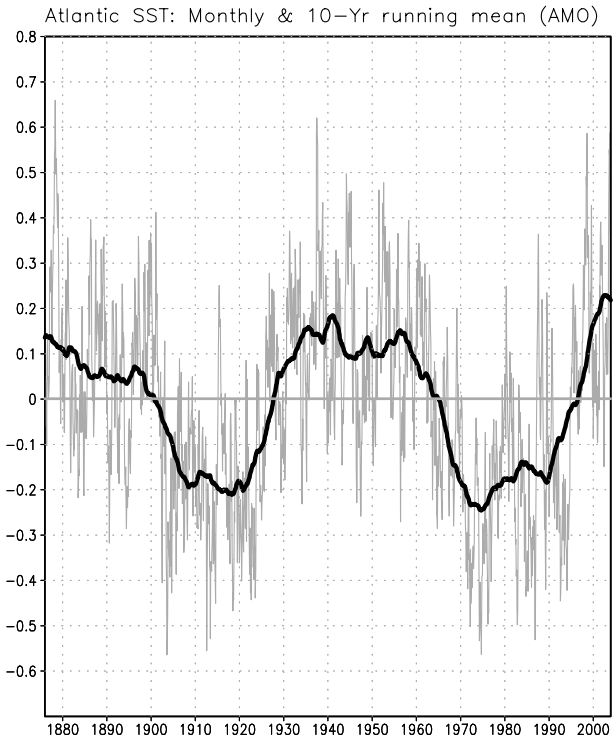

Fig. 1. AMO time series as obtained from the linearly detrended SST Anomalies (°C) averaged over the entire North Atlantic (0°-70°N, 80°W-10°E) calculated using the 10-year running mean (black line). Monthly anomalies are shown by the grey line. SSTs are obtained from the HadISST data set (Rayner et al., 2003).

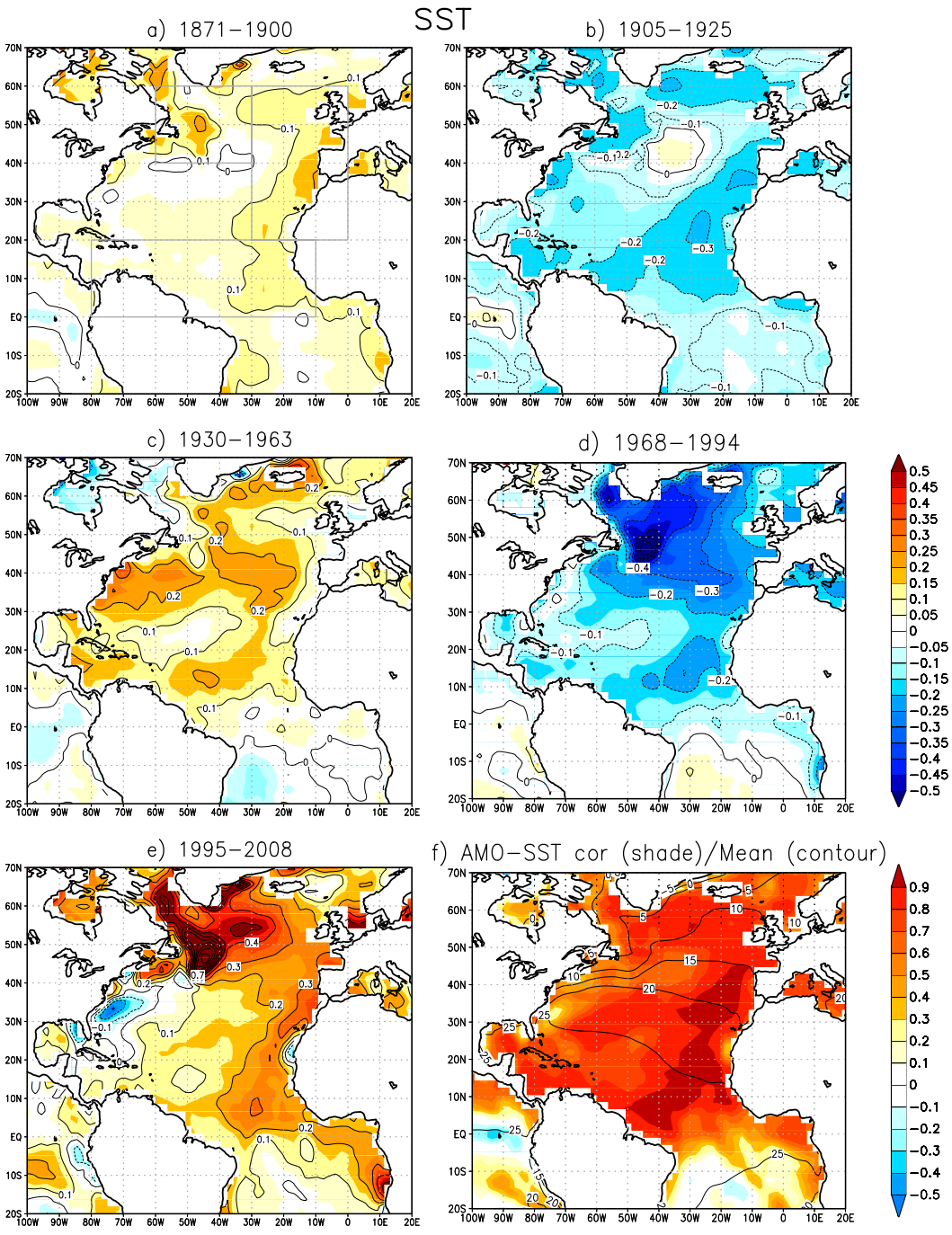

Fig. 2. The sea surface temperature anomalies relative to the 1871-2008 average for the periods (a) 1871-1900, (b) 1905-1925, (c) 1930-1963, (d) 1968-1994 and (e) 1995-2008. The three positive-phase AMO periods are shown in (a), (c) and (e), and the negative phase periods in panels (b) and (d). The anomalies, based on de-trended data, are shown as both contours (interval is 0.1 °C) and shading (interval of 0.05, scale on right of panel d). (f) Long term mean SST (contoured interval 5°C) and the correlation between the AMO and the 10-year running mean SST (shading interval 0.1, scale on right of panel f).

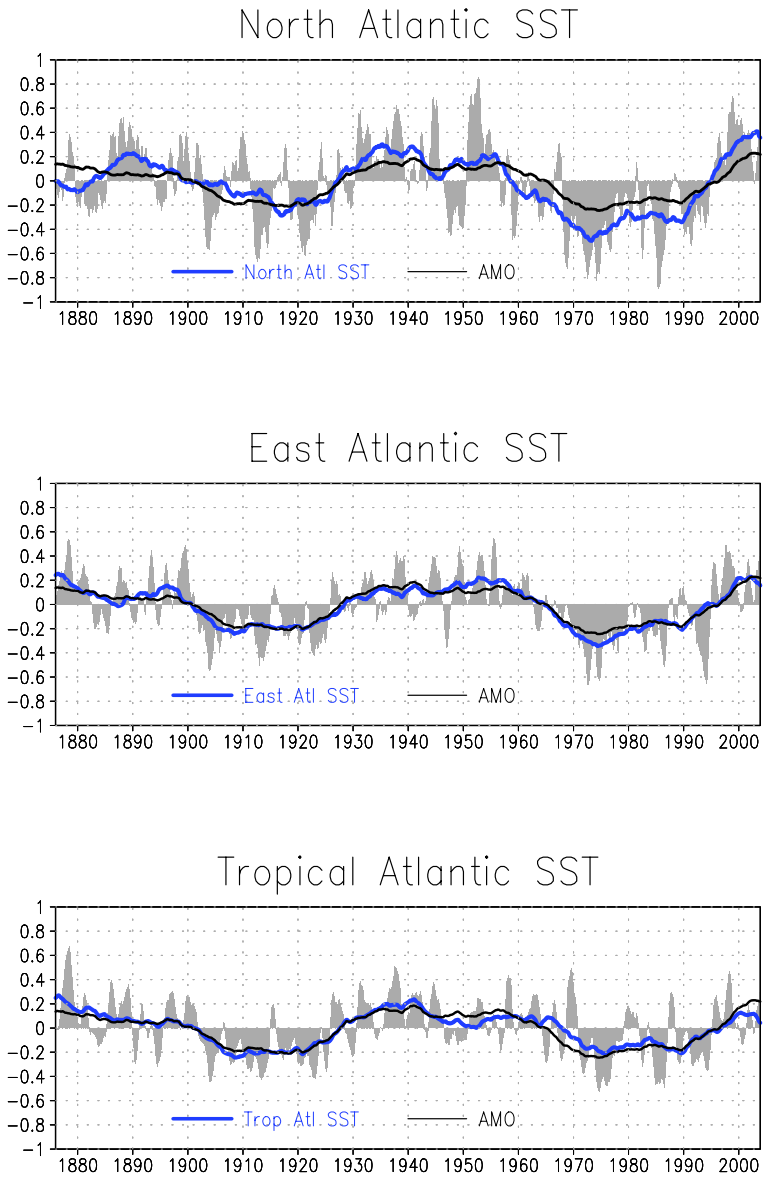

Fig. 3. SST anomalies (°C) averaged over the North Atlantic (40°-60°N, 60°-30°W), Eastern Atlantic (20°-60°N, 30°W-0°) and tropical Atlantic (0°-20°N, 80°W-10°W) regions (gray rectangles in Fig. 2a): 12-month running mean (grey shading), regional 10-year running mean and AMO time series

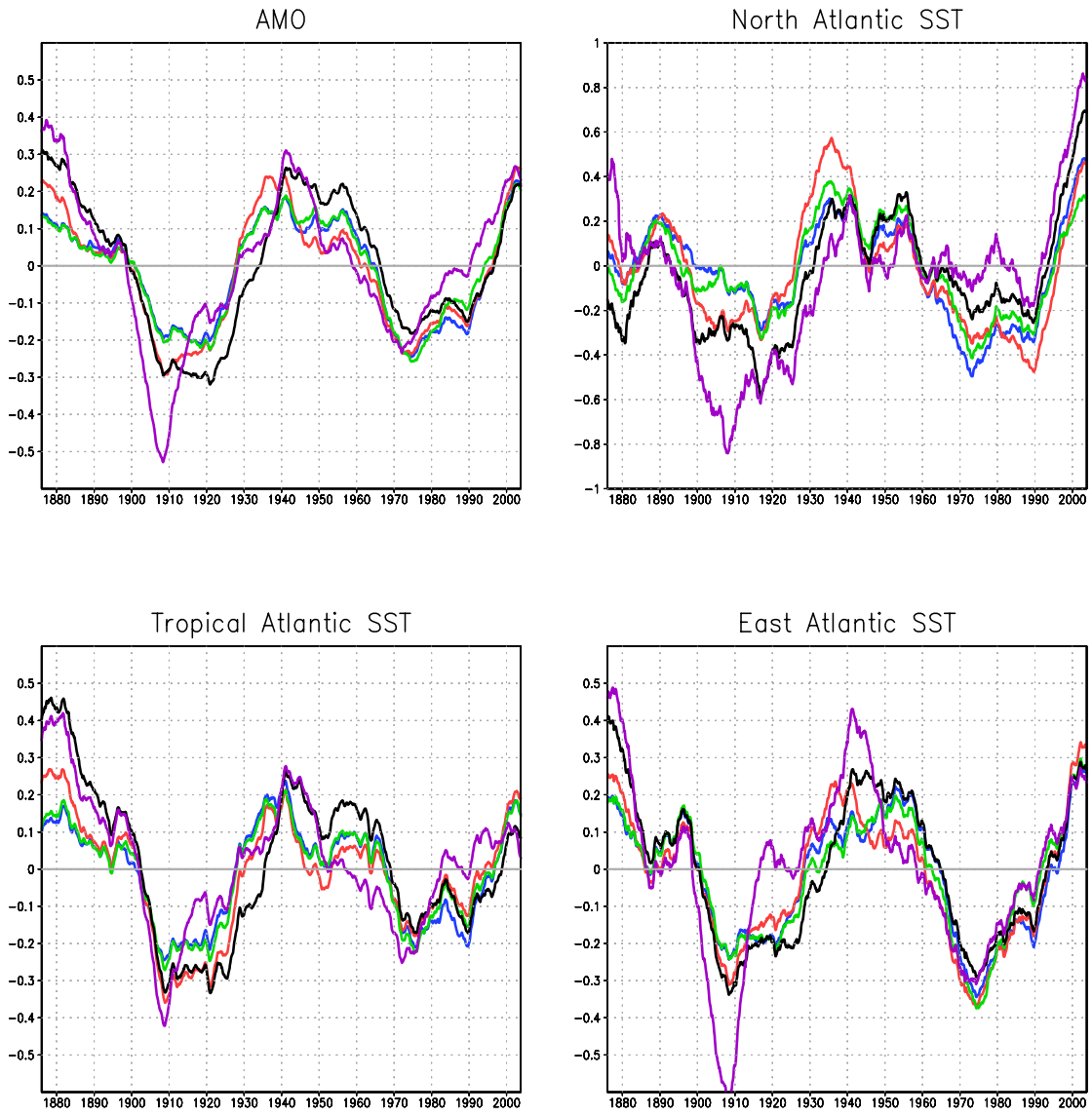

Fig. 4. Time series of the AMO and the de-trended 10-year running average of SST anomalies in the Tropical Atlantic, East Atlantic and North Atlantic regions from the following datasets: HadISST (blue, reference); ERSST (red); Kaplan (green); ICOADS (black). Also shown are the anomalous air temperature time series (purple) averaged over the entire North Atlantic (AMO region) as well as for the three smaller regions. The datasets are described in section 2.

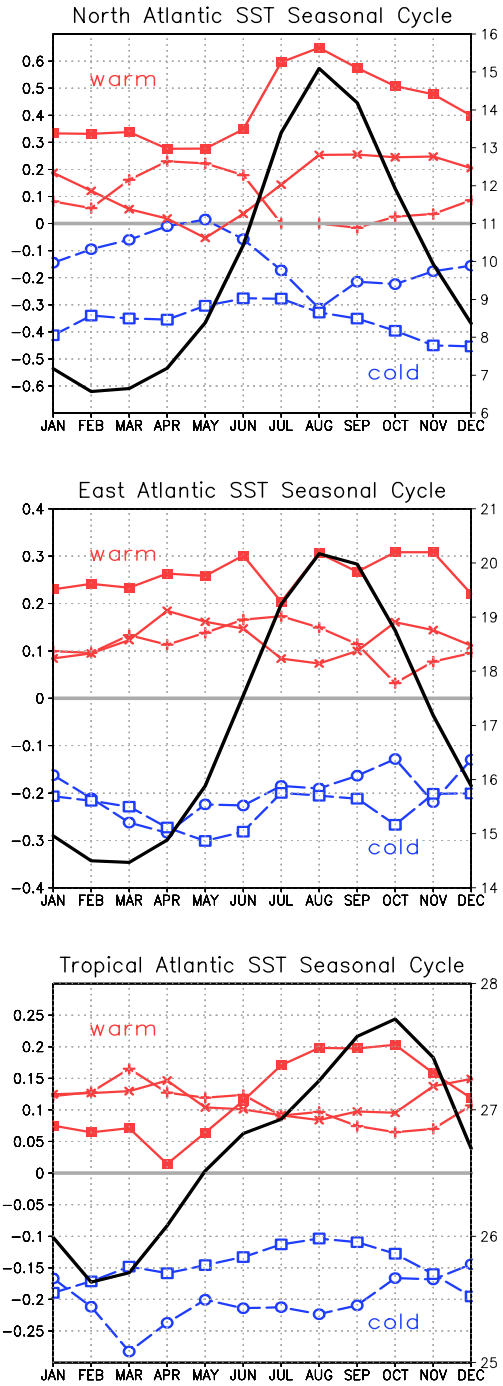

Fig. 5. The seasonal cycle of the long term mean SSTs and the average SST anomalies in each of the 5 epochs in the Tropical, East and North Atlantic regions. The mean SSTs (black line without symbols, scale on right) are based on monthly values averaged over 1871-2008. The unfiltered monthly SST anomalies during the warm epochs (solid lines): 1871-1900 (+), 1930-1963 (**x**), 1995-2008 (■), and cold epochs (dashed lines): 1905-1925 (**O**) and 1968-1994 (□), with the scale on the left. Note the scales of both the mean and epoch anomalies differ between regions.

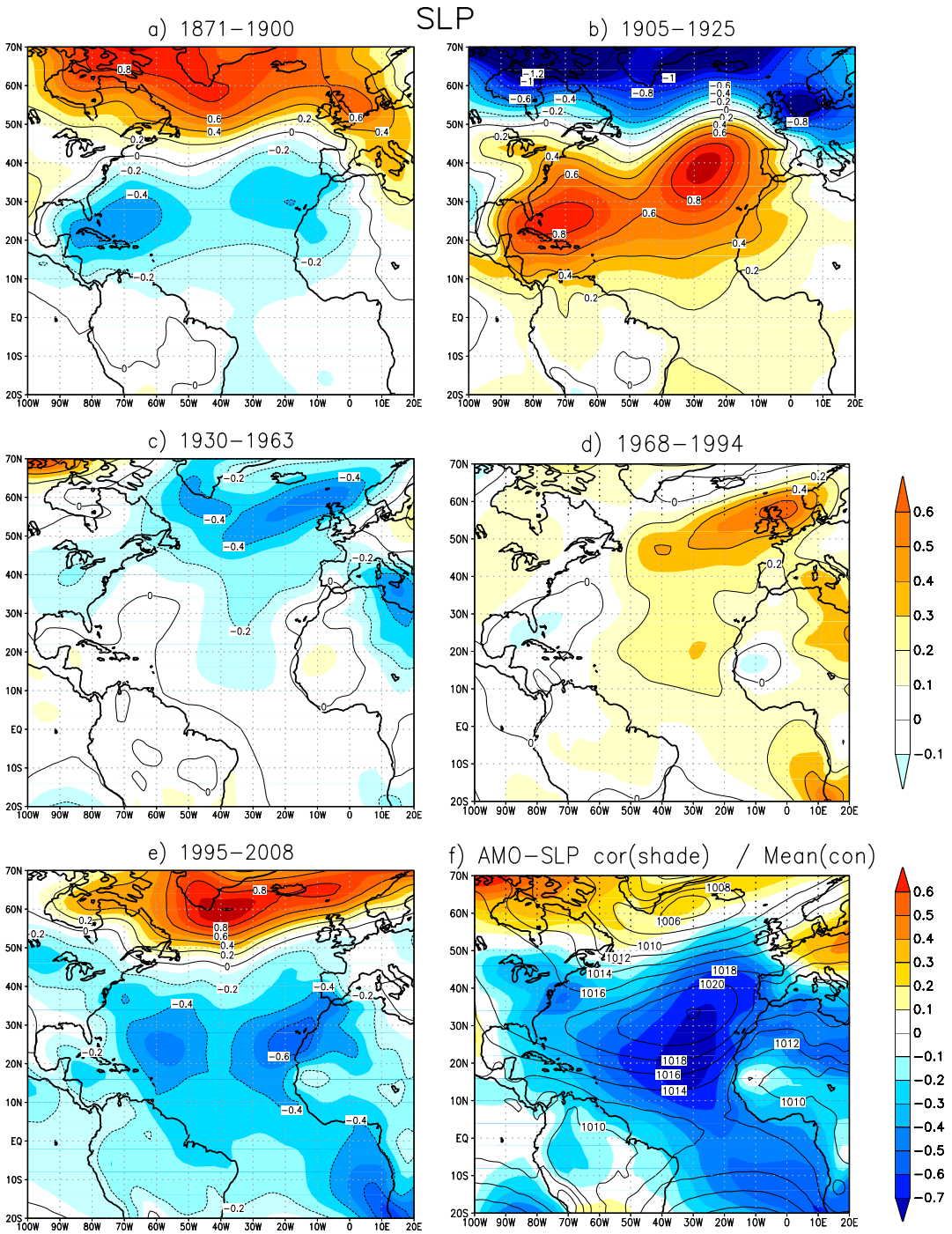

Fig. 6. As in Fig. 2, but for SLP anomalies. The anomalies are shown as both contours (interval is 0.2 mb) and shading (interval of 0.1 mb, scale on right of panel d). (f) Long term mean SLP (contours interval 4 mb) and the correlation between the AMO and the 10-year running mean SLP (shading interval 0.1, scale on right of panel f).

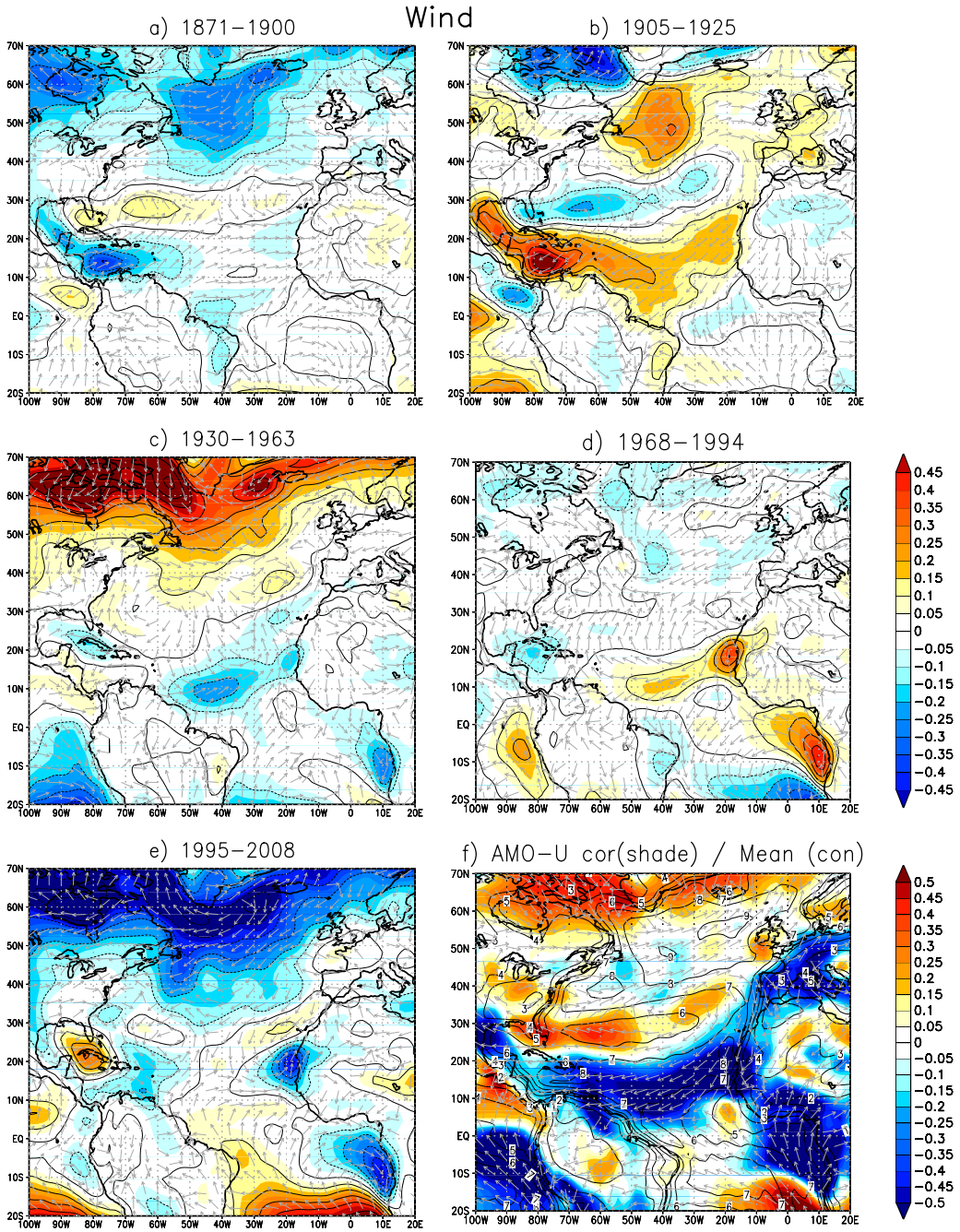

Fig. 7. As in Fig 2 but for the surface wind. (a)-(e) anomalous wind direction (gray equal length vectors) and anomalous wind speed shown by both contours (0.1 m sec) and shading (scale to the right of panel d 0.05 m/sec) for the five periods. (f) Mean wind direction (grey vectors, mean wind speed (contours), correlation between the AMO and the 10-year running mean wind speed (shading, scale on right).

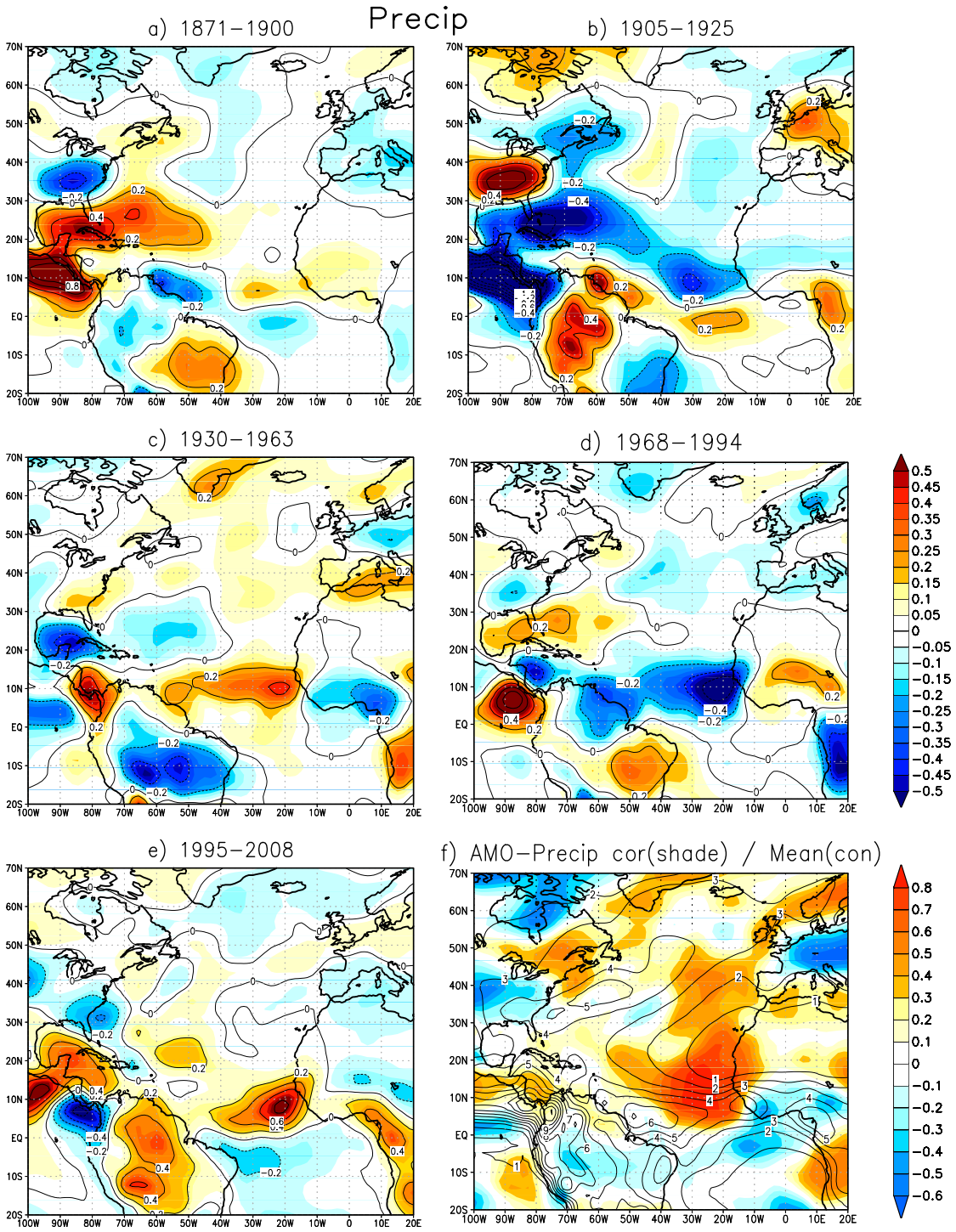

Fig. 8. As in Fig. 2, but for the precipitation. The anomalies are shown as both contours (interval is 0.2 mm day^{-1}) and shading (interval of 0.05 mm day^{-1}, scale on right of panel d). (f) Long term mean precipitation (contours interval 1 mm day^{-1}) and the correlation between the AMO and the 10-year running mean precipitation (shading interval 0.1, scale on right of panel f).

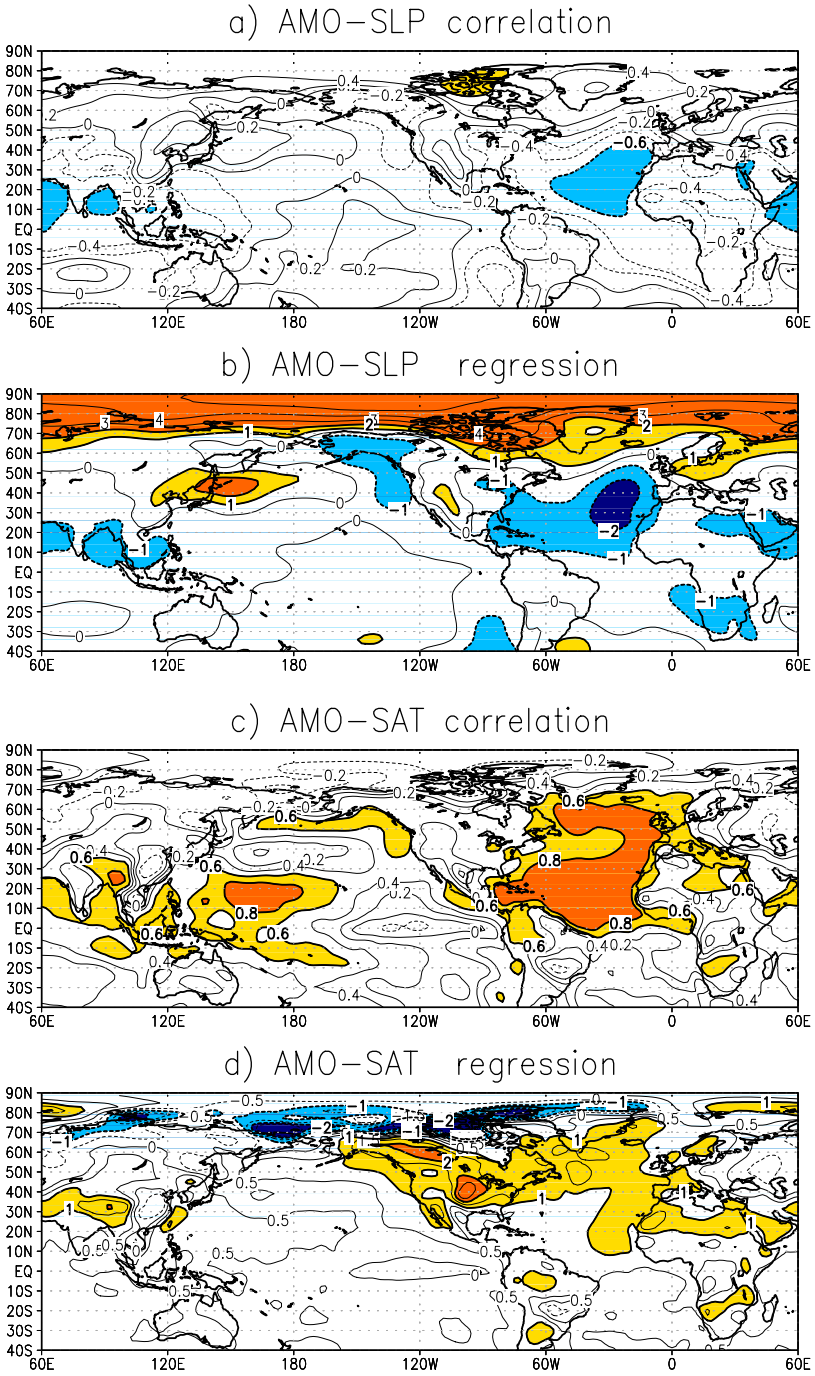

Fig. 9. Correlations between the AMO index and (a) sea level pressure (SLP) and (c) surface air temperature (SAT); regressions of (b) SLP and (d) SAT on the AMO. All variables have been de-trended and smoothed with a 10-year running. The contour intervals are (a) 0.2, (b) 1.0 mb $°C^{-1}$, (c) 0.2, and (d) 0.5°C per $°C^{-1}$ change in the AMO. Absolute correlation (regression) values of 0.6 and 0.8 (1 and 2) are shaded and have thicker contour lines.